

# Scanning probe microscopy of intrafibrillar crystallites in calcified collagen

D. ERTS\*, L. J. GATHERCOLE, E. D. T. ATKINS†

*H. H. Wills Physics Laboratory, University of Bristol, Tyndall Avenue, Bristol BS8 1TL UK*

Vertebrate mineralized tissues are composite materials formed by the organized growth of carbonated apatite crystals within a matrix of collagen fibres. Calcified collagen from turkey tendon was investigated using scanning tunnelling microscopy (STM) and atomic force microscopy (AFM). Samples were treated with hydrogen peroxide to enhance the mineralized phase by removing part of the collagen matrix and the results compared with the untreated material. Plate-like crystalline entities with dimensions  $35 \text{ nm} \times 5\text{--}8 \text{ nm}$  by  $\sim 1.5 \text{ nm}$  were seen. These dimensions are consistent with previous reports using transmission electron microscopy (TEM) of calcified tendon and topographic imaging of tendon crystals. The resolution of the images obtained using STM is better than the previously reported pictures obtained using TEM or scanning electron microscopy (SEM). The value of  $35 \text{ nm}$  is the same as the gap region in the structure of the collagen fibrils. Stacking of plates and plate-aggregates are a dominant feature in the scanning images. These results support the concept of organized intra-fibril mineral crystals within the organic collagen matrix. Electron diffraction and X-ray diffraction were undertaken on the samples and the patterns recorded match those previously reported for carbonated apatite.

## 1. Introduction

Tendons are strong, relatively inextensible structures composed largely of type I collagen molecules. The collagen molecules themselves are rods  $300 \text{ nm}$  long and  $1.5 \text{ nm}$  diameter, composed of three intertwining polypeptide chains [1]. The molecules associate in the first instance by juxtapositioning into pentamers, with a defined relative axial stagger to generate a long elementary fibre, the integrity of which is maintained by substantial regions of mutual overlap between adjacent molecules. In addition, gaps occur in the structure of length  $35 \text{ nm}$  [1]. These microfibrils coalesce to form fibrils [2] and within the overall three-dimensional architecture several  $35 \text{ nm}$  gap regions can be contiguous, thereby creating plate-like channels  $\sim 1.5 \text{ nm}$  wide and  $35 \text{ nm}$  long in the direction to the collagen molecular axis. Depths of the order  $10 \text{ nm}$  have been implied [3]. It is into these sites that carbonated apatite mineralization occurs in the leg tendons of some large birds, the turkey being the best studied [4–8] because it provides a good model for the early stages of bone mineralization.

Many difficulties arise in the study of the structure and processes in calcified tissues. The materials themselves are complex, the mineral component heterogeneous, variable and poorly crystallized. Calcified turkey tendon has become a material of choice for such studies since the local parallelism of the collagen fibres, as opposed to the orientational complexities in bone, together with a typically less dense calcification, makes analysis easier.

The visualization of these small crystals needs a microscopy capable of high resolution. Previous investigations have used transmission electron microscopic techniques, [5, 9, 10] including selected area dark field imaging and spectroscopy [7, 11], electron diffraction [12] and topographic imaging [13]. Even if 'wet' samples are quenched-cooled the images are subject to distortion in the high vacuum of the electron microscope, and electron beam damage to the specimens occurs, since these are unstained and un-fixed [13].

To date the main biophysical techniques, transmission and scanning electron microscopies (TEM and SEM), X-ray diffraction and optical microscopies have not solved the structural problems since separation of the two components without alteration of one or the other has not been achieved. Scanning probe microscopy (SPM), however, holds out the promise of simultaneous study of the two components since these techniques can image hard and soft components equally well [14, 15].

As a first step in the application of these techniques to calcified tissues, we present here the first SPM images of isolated apatite crystals from calcified turkey tendon at resolution greater than those so far achieved by TEM.

Fig. 1 shows a schematic diagram of the sequence of events in the initiation of calcification in turkey tendon, mainly summarized from the studies of Traub and co-workers [3, 9–13]. It shows a widely held consensus view of these early events largely detected

\* *Permanent address:* Department of Condensed Matter, Chemical Physics, University of Latvia, 19 Rainis Blvd, 226098 Riga, Latvia.

† To whom correspondence should be addressed.

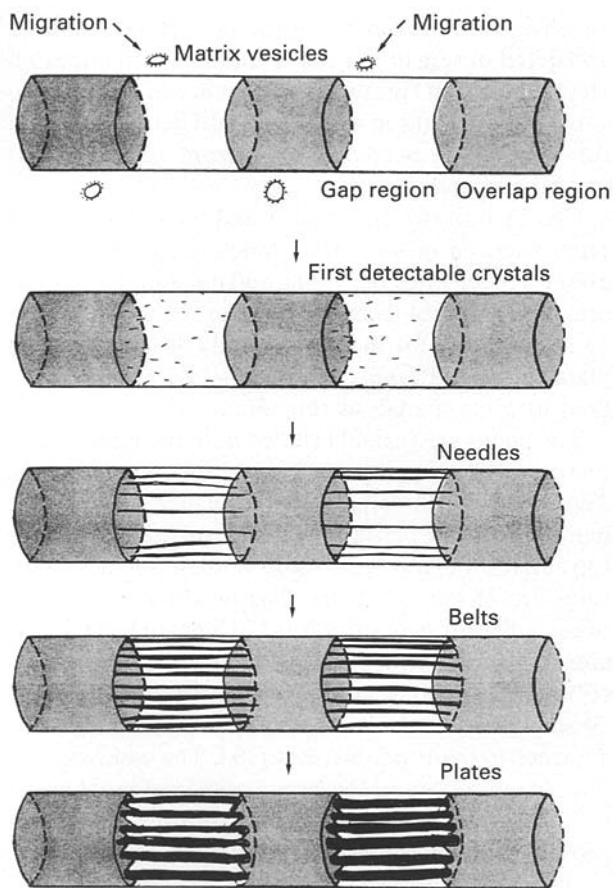


Figure 1 Diagram of the sequence of events in early crystallization of intrafibrillar hydroxyapatite in the turkey tendon.

by TEM. Matrix vesicles holding strong solutions of calcium and phosphate ions are secreted in the matrix and approach the collagen fibrils. As these disappear, the first crystals are detected in the gap regions. Though discovered as long ago as 1957 by Fitton-Jackson [16] this stage has been difficult to discern and has only recently been unequivocally confirmed [9]. The early crystals then coalesce into needle-like, then belt-like entities and eventually grow into plates. These plates can develop further and occupy molecular overlap as well as gap regions in the collagen fibrils [10].

In this investigation we have used the newer techniques of SPM, in particular scanning tunnelling microscopy (STM) and atomic force microscopy (AFM) to study calcified turkey tendon. Using SPM we can examine the surface topology of suitable specimens at atomic resolution by scanning a fine probe—a tip—over the surface. We are able to record the surface profile in air or under water. In order to preferentially enhance the imaging of the apatite crystals we prepared samples which had been treated with hydrogen peroxide for various times, which removed part of the collagen matrix, allowing better visualization of the crystals.

## 2. Materials and methods

### 2.1. Scanning probe microscopy

The structure used as a model for mineralized collagen was calcified turkey tendon. There are well-established precedents for taking this as a model for bone calci-

fication in which the intra- and interfibrillar mineral may be more readily visualized than bone itself, owing to less extensive mineralization and simpler crystallite orientation. However, it probably shares the same organizational motifs of bone calcification, particularly the layering of carbonated hydroxyapatite crystal aggregates [4–8].

In the first experiments, the fully calcified regions of 20-week-old turkey leg tendons were cut finely into sub-millimetre pieces by bone cutters and ground finely in a pestle and mortar, either at 4 °C in water, or at liquid nitrogen temperatures and subsequently suspended in water. After the larger particles were allowed to sediment under gravity for 30 min, the slightly cloudy supernatant was pipetted and a 50–100 µl drop placed on freshly cleaved graphite (HOPG grade 'A' or 'B'. Union Carbide Inc., Cleveland, Ohio) and allowed to evaporate. Specimen surfaces were then washed once or twice with highly purified distilled water (molecular biology grade—BDH/Merck) and either examined in a STM (WA Technology, Cambridge, UK) or subjected to further treatment to enhance the imaging of the mineral phase. In these cases the dried surface was etched either for 5 min or 45 min at room temperature with a drop of 20 volumes hydrogen peroxide. This had the effect of substantially removing the organic, collagenous material, but leaving the inorganic crystallites intact and *in situ* for more detailed imaging. The substrate also appeared unaffected by this treatment. The peroxide treatment was terminated by flushing with an excess of purified water. This process left adequate amounts of calcified material adhering to the graphite for easy location and imaging of the material.

Scanning conditions were similar to those used previously for imaging collagen [17]. That is, medium bias voltage of about 500 mV and a tunnel current of about 50 pA; typical image acquisition times of 1 min 49 s to 3 min 38 s were commonly used.

For AFM experiments, a Nanoscope III microscope (Digital Instruments, Santa Barbara) was used in contact mode with a multimode head and using micro-prefabricated cantilevers with integral silicon nitride tips. The Nanoscope III image processing package was used to provide section analysis of the STM images. The image files were first converted from the WA to Nanoscope format.

In order to keep the forces on the crystallites as low as possible, cantilevers of low spring constant ( $K = 0.06 \text{ N m}^{-1}$ ) were used, the operating range of the AFM being determined by the lowest force at which constant and stable cantilever deflection images could be obtained. Specimens were scanned in air and in water.

Specimen preparation was similar to that of the STM experiments except that freshly cleaved mica surfaces were used. Thin sheets of mica (Agar Aids, plc) were fixed by cyanoacrylic glue to magnetic stainless steel discs for assembly in the AFM.

### 2.2. X-ray diffraction

Some of the samples prepared for SPM and treated with hydrogen peroxide were packed into a sealed

thin-walled glass tube for X-ray diffraction experiments. The samples were X-rayed with nickel filtered  $\text{CuK}\alpha$  radiation. An evacuated flat plate camera and pinhole collimation was used. The patterns were calibrated by dusting calcite externally on the walls of the specimen tube.

### 2.3. Selected area electron diffraction

Specimens were prepared on carbon coated grids in an identical manner to those used for the SPM investigation. Electron diffraction patterns were obtained using a Philips 301 transmission electron microscope in diffraction mode.

## 3. Results

We have observed a wide range of structures in the specimens with the three types of treatment (untreated, 5 min and 45 min  $\text{H}_2\text{O}_2$  etched). We rejected all images occurring near steps and other defects in the graphite and all images resembling published artefacts [18] and others known to us. We also rejected all images showing an apparent height maximum under 1 nm.

Though both collagen fibrils and hydroxyapatite crystals could be seen in untreated material, there was

an obvious improvement in the resolution definition and detail observable in the crystallites with increased  $\text{H}_2\text{O}_2$  treatment, presumably as more of the organic content of the tendon was removed. Therefore most of the material presented here is from 45 min  $\text{H}_2\text{O}_2$  treated specimens.

Fig. 2a, b shows the top view and three-dimensional representation of structures which are aggregates of about  $170 \times 95$  nm (left)  $200 \times 60$  nm (middle) which are composed of trapezoid plates of surface sizes  $35 \times 35 \times 18$  nm for the most prominent free-standing plate (Fig. 2c, d) and of heights  $\sim 1.5$  nm, as measured by section analysis (Fig. 3).

The plates are variably shifted and overlapped relative to each other by 10–25 nm, and tilted (Fig. 3). They show a well-defined finer structure consisting of markedly parallel striations which protrude from the top surface. Lateral dimensions of these smaller structures are  $35 \text{ nm} \times 5\text{--}8 \text{ nm}$ . The height variation between adjacent structures is 0.2–0.5 nm. The length is commensurate with the known length of the type I collagen fibril gap region [2] where calcification and crystal formation is thought to be initiated [7–13] adjacent to hydrophobic sites [19]. The widths of the fine structures are in the range of diameters of either collagen penta-fibrils or 8 nm microfibrils. It has not proved possible to resolve the fine structure further,

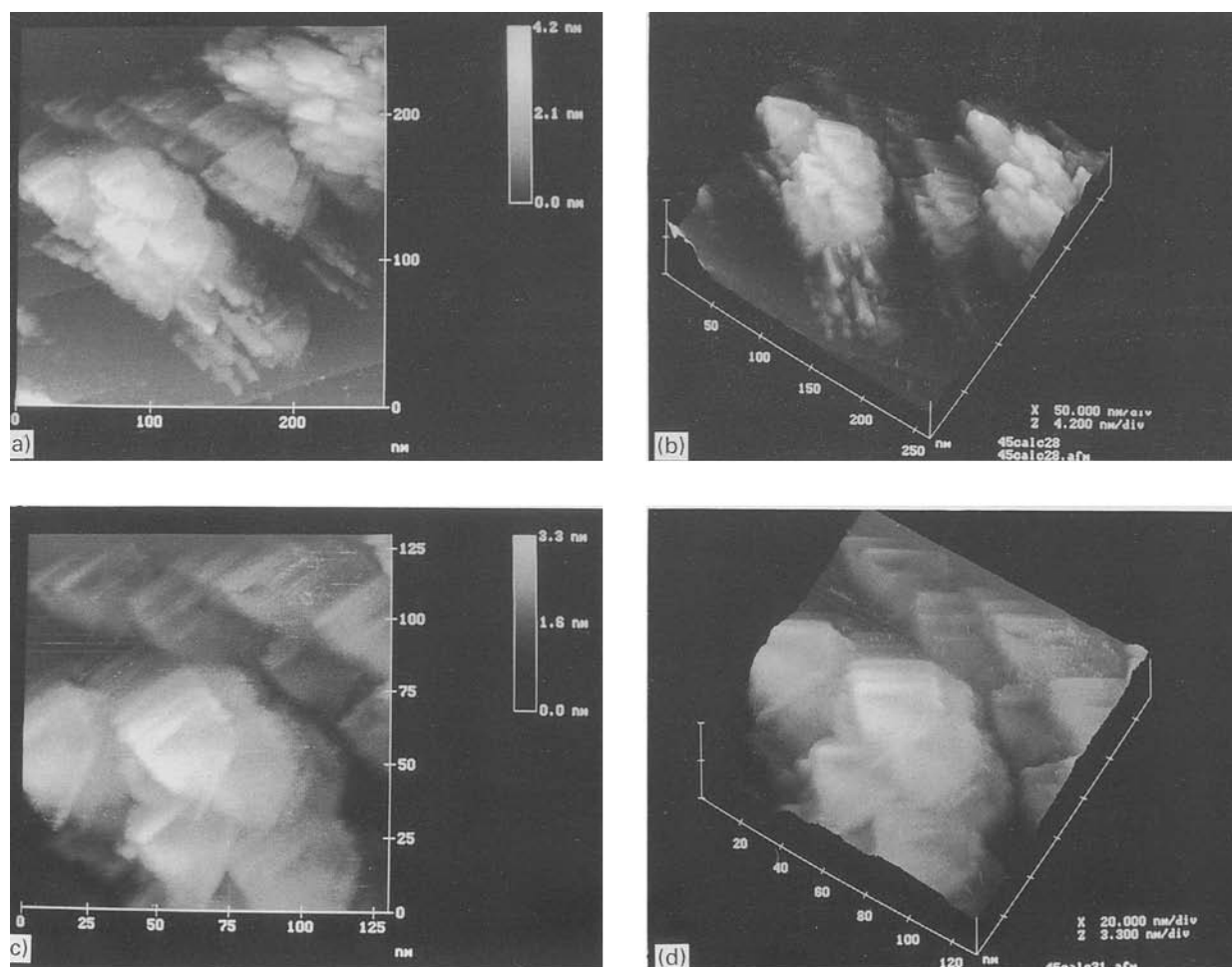


Figure 2 STM top views (a, c) and corresponding surface plots (b, d) of calcified turkey tendon treated with hydrogen peroxide for 45 min. Plate-like aggregates with dimensions  $\sim 35$  nm are seen. (c) and (d) are higher magnification of a selected part of the more general field of view shown in (a) and (b). Bias voltage 800 mV, tunnelling current 50 pA.

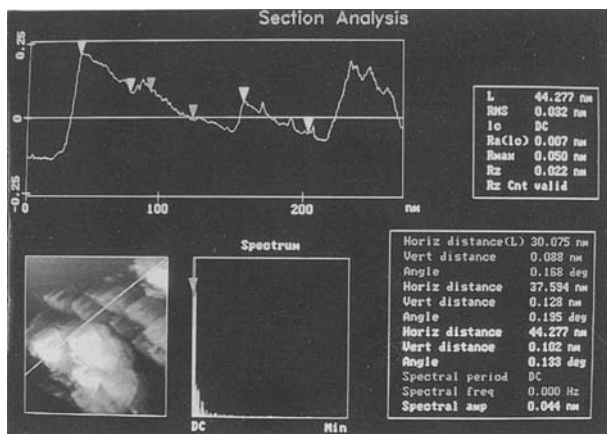


Figure 3 STM top view of the hydroxyapatite crystals together with a cross-sectional trace profile highlighting the periodicity  $\sim 35$  nm. The specimen treatment and scanning conditions are the same as Fig. 1.

but it is possible that it represents the surface feature of extra stacking of platelet subunits. The height of the trapezoid plates is of the same order as the diameter of collagen molecules, which might well be expected if they are located between adjacent molecules *in situ* (Fig. 4). Alternatively the whole trapezoid plate may be solid, with only the surface features representing the impression of etched-out collagen molecules.

Fig. 5a, b exhibits plate-like entities and thicknesses estimated at 1.5 nm. Fig. 5c, d highlights the substantially different orientations of the crystallites that can occur.

Fig. 6 shows what appears to be views of corners and edges of stacked platelets, again highlighting a dimension of 35 nm. We noticed on occasions that this texture mapped onto a curved, almost cylindrical

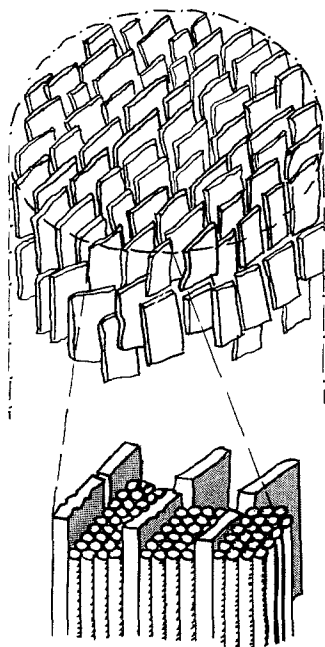


Figure 4 Schematic diagram of the arrangement of plate-like hydroxyapatite crystals in a mineralized turkey tendon collagen fibril, showing the collagen molecules between the plates (redrawn from Weiner and Traub [3]).

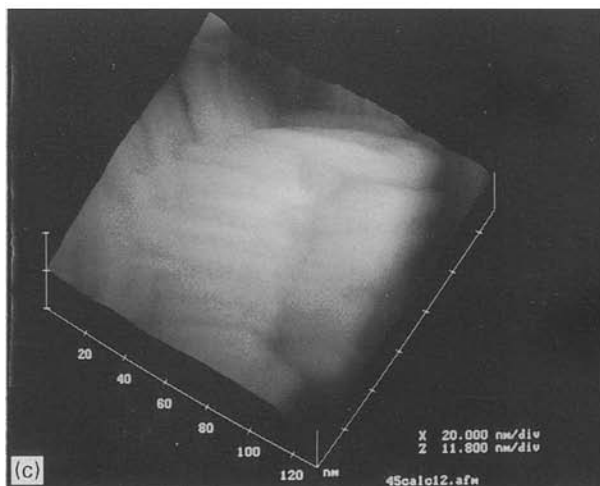
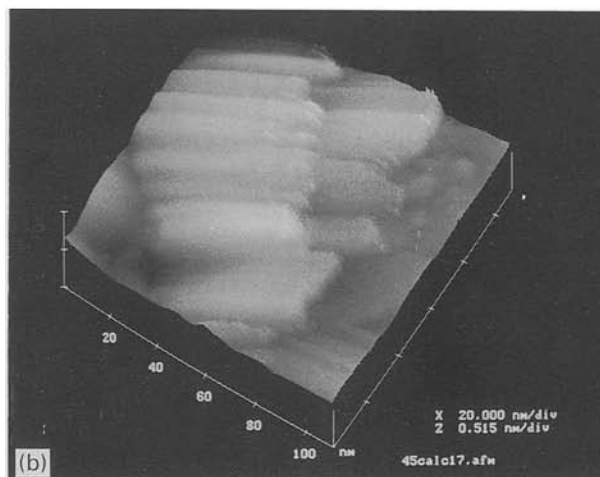
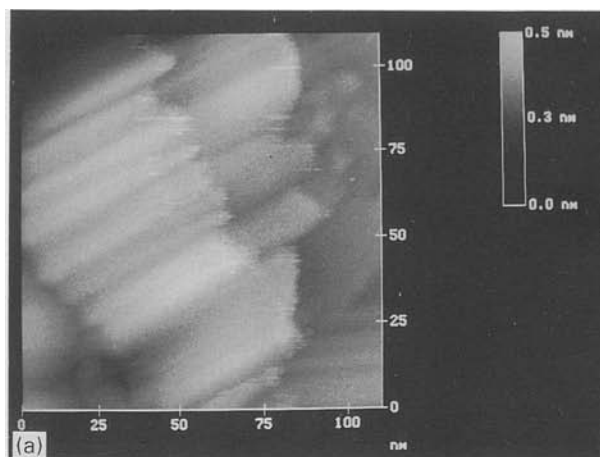


Figure 5 STM top view (a) and corresponding surface plots (b, c) of the plate-like stacks almost edge-on. A single plate with an estimated thickness  $\sim 1.5$  nm (b). Image (c) shows that the aggregates of crystals can have neighbouring aggregates with different orientations. Treatment conditions: 45 min in hydrogen peroxide prior to washing. Bias voltage 800 mV, tunnelling current 60 pA.

architecture (see Fig. 6c) which could be related to the belt-like crystal arrays that have reported previously [10]. We have also observed periodicities smaller than 35 nm.

Untreated samples of pulverized calcified turkey tendon also show areas where the dimensions are less than 35 nm (Fig. 7a, b, c). In particular Fig. 7a shows

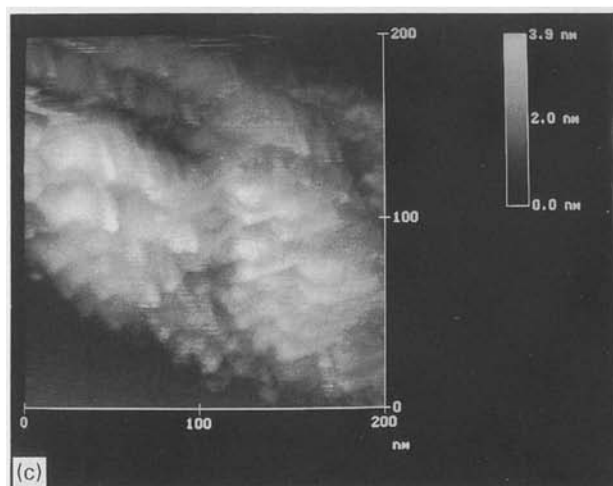
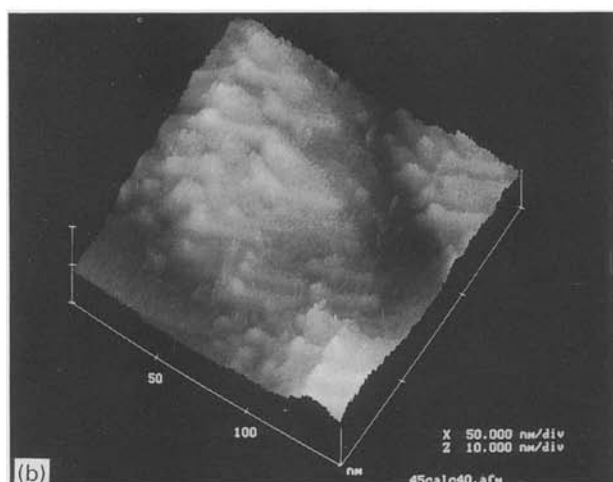
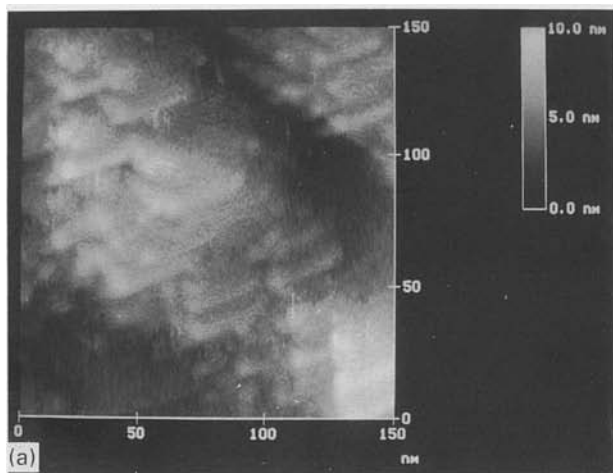


Figure 6 STM top view (a, c) and surface plot (b) of calcified turkey tendon treated for 45 min in hydrogen peroxide prior to washing with water. Corners and edges of the 35 nm plate-like stacks are imaged. In the lower magnification image (c) of an adjacent region of the sample the tendency for the aggregates to follow a curved bulk topology can be seen.

periodicity  $\sim 8$  nm in the anticipated direction of the plates and 5 nm in the orthogonal direction.

In the STM work, all images were taken on a graphite substrate and so it was thought prudent to obtain additional images on a mica substrate using

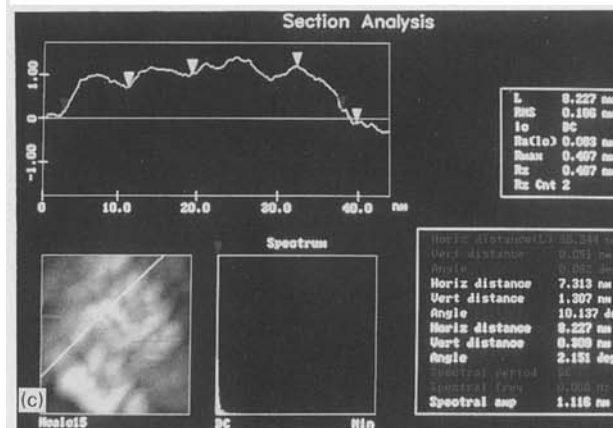
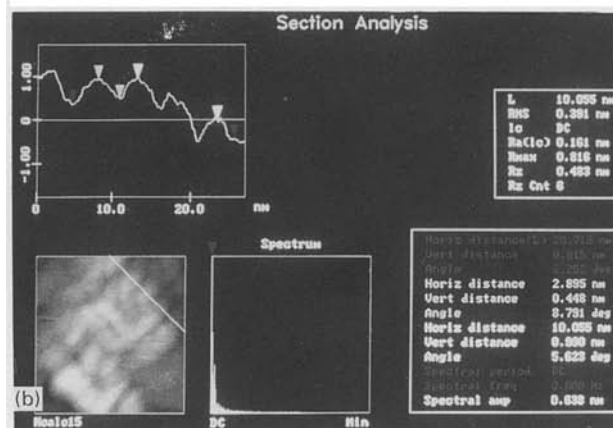
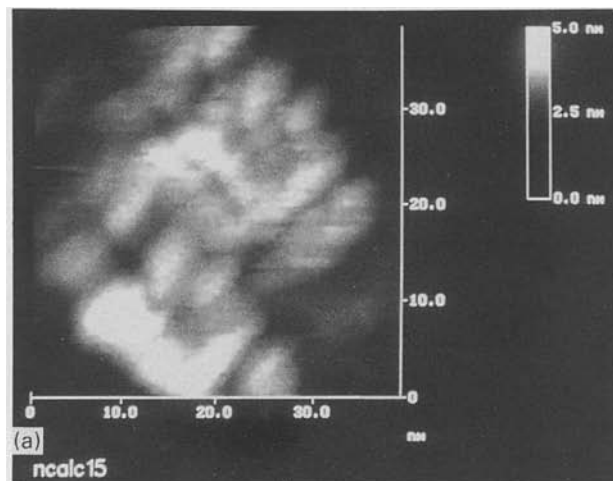


Figure 7 (a) STM top view of untreated calcified turkey tendon. Again substructure of the 35 nm dimension can be seen. (b) The cross-sectional trace profile along a diagonal line, (c) The cross-sectional trace profile along a different diagonal. Bias voltage 600 mV, tunnelling current 100 pA.

AFM. Although the resolution achievable was not as good as that with STM, plate-like entities of the length  $\sim 35$  nm were seen. A representative picture and line profile are shown in Fig. 8a, b.

Fig 9a, b shows the electron diffraction and X-ray diffraction pattern, respectively, for the peroxide treated samples. The spacings of the prominent rings are listed in Table I and compared with those of Bigi *et al.* [20].

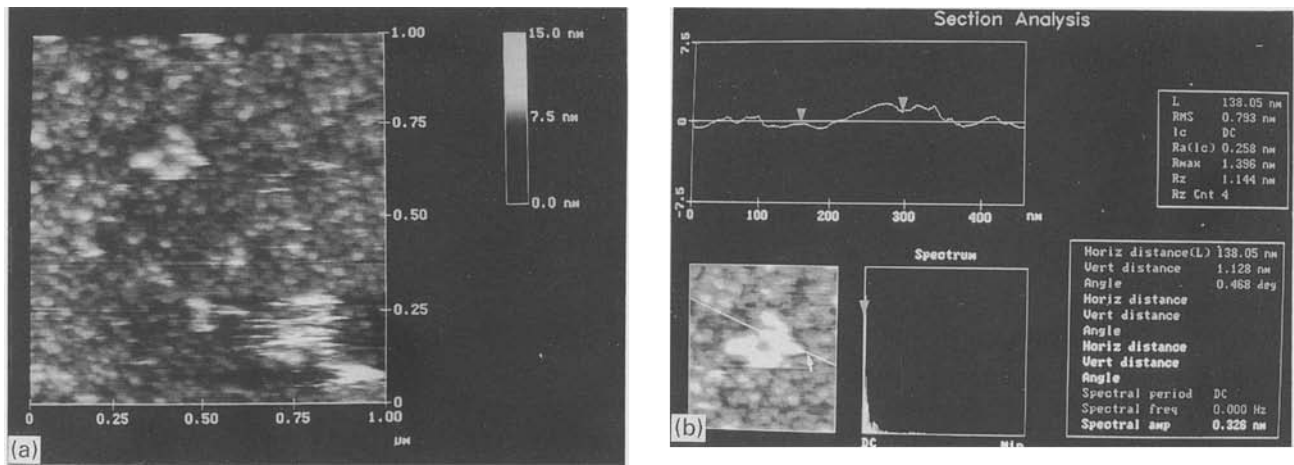


Figure 8 (a) AFM top view of calcified turkey tendon treated for 45 min with hydrogen peroxide and deposited on a cleaved mica substrate. (b) Shows a cross-sectional trace profile of a localized area. The periodicity of  $\sim 35$  nm is evident. Scan rate 3.3 Hz, spring constant of cantilever  $0.06 \text{ N m}^{-1}$ . Set point  $-6.7 \text{ V}$ .

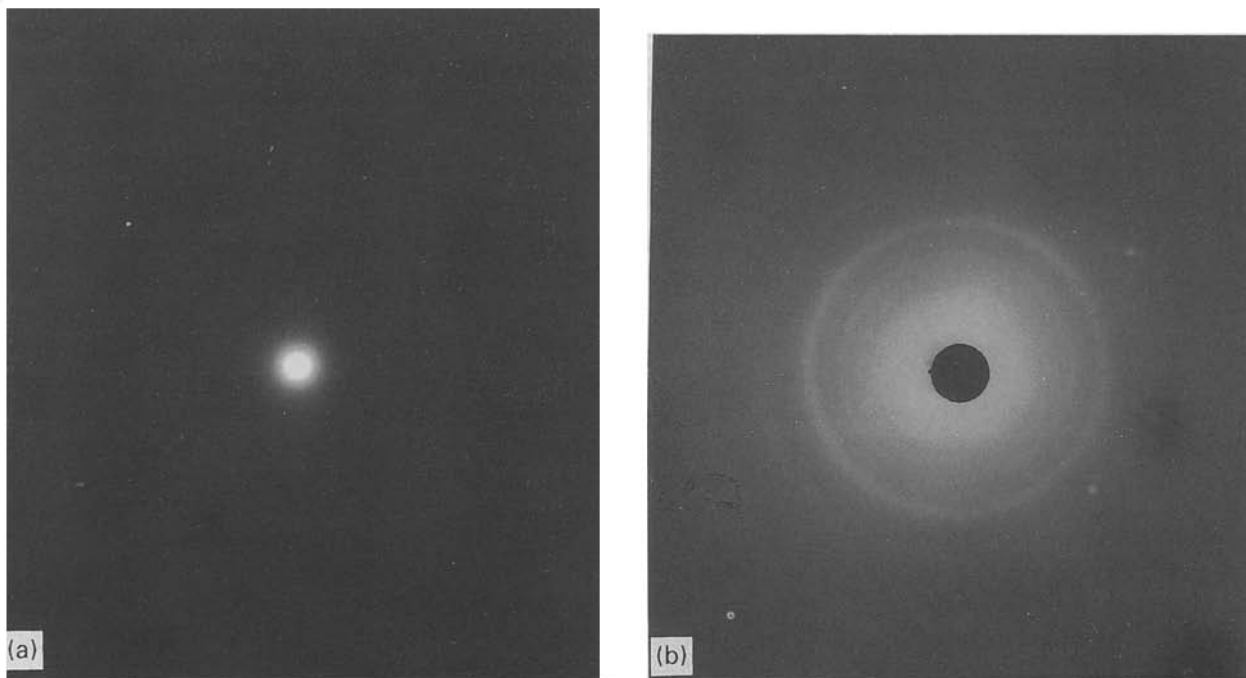


Figure 9 (a) Selected area electron diffraction image of crystals from turkey tendon prepared in the same way as for SPM. See spacings given in Table I. (b) Wide angle X-ray diffraction pattern of a large proportion of the tendon crystals.

TABLE I Diffraction spacings measured in nanometers

| Electron diffraction | X-ray ( $\pm 0.005$ ) | X-ray [20] | Comments                    |
|----------------------|-----------------------|------------|-----------------------------|
| 0.342                | 0.334                 | 0.344      | Strong, partial orientation |
|                      | 0.309                 | 0.308      | Weak, partial orientation   |
| 0.274                | 0.278                 | 0.278      | Very strong and broad       |

#### 4. Discussion and conclusions

The electron diffraction and X-ray diffraction results of the peroxide treated samples match that of those for carbonated apatite reported by Bigi *et al.* [20] as listed

in Table I. The three prominent reflections have similar spacing, intensity and degrees of orientation. The first diffraction ring is consistent with the reported 002 reflection from the hexagonal phase of carbonated apatite ( $a = 0.941 \text{ nm}$ ,  $c = 0.688 \text{ nm}$  [20]). Thus we are confident that the crystalline entities we observe using the SPM techniques are indeed crystalline platelets of carbonated apatite.

Scanning probe microscopy (SPM) of preparations of calcified tissue reveal architectures wholly consistent with current ideas concerning the mineralization of collagen tissues. Furthermore the images provide greater resolution than previously attained using other biophysical structural techniques such as transmission and scanning electron microscopies [5, 9, 10, 21] X-ray diffraction [20, 21] and electron diffrac-

tion [12, 22] regarding the crystallites in calcified turkey tendon.

The SPM techniques have demonstrated a clear potential for improved imaging in this field by enabling the small crystals of hydroxyapatite to be visualized in the material either in air or immersed in water. The STM technique in particular can provide the dimensions of individual plate-like crystallites from images (Figs 1 and 2) whereas, in general, these can only be inferred from TEM of different crystallites which happen to be lying edge-on or flat-on. Our images of the plates are in good agreement with the diagrams drawn by Weiner and Traub [3] deduced from their TEM data in unstained turkey tendon collagen fibrils. The length of 35 nm for the plates is a common dimension, but as indicated from previous TEM studies [3, 13] layer structures and aggregates are also observed. The stacking of the plates is predicted from TEM studies, though in this study we have not been able to image the collagen and mineral together *in situ*.

Junctions of a near-orthogonal nature between plate stacks are also seen, and though it is not yet known how these relate to arrangements in the unpulverised tendon, it is interesting to compare our Fig. 5 with Fig. 5 of Weiner and Traub [3] showing a diagram of lamellae of stacked plates crossing in bone.

Our images bear the closest relationship to the previously reported TEM topographic images of disaggregated tendon crystals [13]. We used very similar preparation procedures, except that we used hydrogen peroxide, because we thought this was less likely to leave any solid deposits, rather than sodium hypochlorite [22] to remove the organic phase. Virtually all the structures and textures discussed in that paper [13] can be identified in our STM images of the plate-like crystals. We have routinely achieved magnifications of the crystals in excess of  $\times 400\,000$  even in these initial studies. Landis *et al.* [13] report beam damage in the mineral and collagen components in their TEM images of  $\times 125\,000$ . It would appear that SPM techniques have a very useful role to play in future biomineralization research.

The TEM evidence frequently suggests 'needles' of 35 nm and shorter in the gap regions of collagen fibrils. It is interesting that some structures we see by STM are commensurate with these and could represent earlier stages in the intrafibrillar calcification released by our pulverization and collagen etching processes.

Clearly a more comprehensive developmental study using varying stages of turkey tendon calcification, and visualizing the collagen component simultaneously is needed.

## Acknowledgements

D. E. wishes to thank the EC TEMPUS programme for supporting a collaborative visit to the University of Bristol. The authors thank the AFRC and MRC for support. The authors are grateful to Dr K. Veluraja for the electron diffraction image shown. L. J. G. thanks professor W. Traub for his encouragement and suggestions.

## References

1. M. E. NIMNI and R. D. HARKNESS, in "Collagen: volume, biochemistry", edited by M. E. Nimni (CRC Press, Boca Raton, 1988) p. 14.
2. J. A. CHAPMAN, M. TZAPHLIDOU, K. M. MEEK and K. E. KADLER, *Electron Microsc. Rev.* **3** (1990) 143.
3. S. WEINER and W. TRAUB, in "Mechanism and phylogeny of mineralization in biological systems", edited by S. Suga and H. Nakahara (Springer-Verlag, Tokyo, 1991) Ch. 2.21, p. 247.
4. M. V. NYLEN, D. B. SCOTT and V. M. MOSLEY, in "Calcification in biological systems", edited by R. F. Sognaes. (A.A.A.S., Washington, D.C., 1960) p. 129.
5. W. J. LANDIS, *J. Ultrastruct. Mol. Struct. Res.* **94** (1986) 217.
6. A. BIGI, A. RIPAMONTI, M. H. J. KOCH and N. ROVERI, *Int. J. Biol. Macromol.* **10** (1988) 282.
7. A. L. ARSENAULT, *Calcif. Tissue Int.* **43** (1988) 202.
8. J. S. SHAH, A. LA MONACA, A. BIGI and N. ROVERI, *Nucl. Instr. Meth.* **A308** (1991) 285.
9. W. TRAUB, T. ARAD and S. WEINER, *Matrix* **12** (1992) 251.
10. *Idem.*, *Connective Tissue Res.* **28** (1992) 99.
11. A. L. ARSENAULT, B. W. FRANKLAND and F. P. OTTENSMEYER, *Calcif. Tissue Int.* **48** (1991) 46.
12. W. TRAUB, T. ARAD and S. WEINER, *Proc. Nat. Acad. Sci. USA* **86** (1989) 9822.
13. W. J. LANDIS, J. MORADIAN-OLDAK and S. WEINER, *Connective Tissue Res.* **25** (1991) 181.
14. M. J. MILES and T. J. MCMASTER, in "STM and SFM in biology", edited by O. Marti and M. Amrein (Academic Press, San Diego, 1993) p. 177.
15. M. RADMACHER, R. W. TILLMANN, M. FRITZ and H. E. GAUB, *Science* **257** (1992) 1900.
16. S. FITTON-JACKSON, *Proc. Roy. Soc. B* **146** (1957) 270.
17. L. J. GATHERCOLE, M. J. MILES, T. J. MCMASTER and D. F. HOLMES, *J. Chem. Soc. Faraday Trans.* **89** (1993) in press.
18. C. R. CLEMMER and T. P. BEEBE, *Science* **251** (1991) 640.
19. M. E. MAITLAND and L. A. ARSENAULT, *Calcif. Tissue Int.* **48** (1991) 341.
20. A. BIGI, L. DOVIGO, M. H. J. KOCH, M. MOROCUTTI, A. RIPAMONTI and N. ROVERI, *Connective Tissue Res.* **25** (1991) 171.
21. D. W. L. HUKINS, in "Calcified tissue", edited by D. W. L. Hukins (MacMillan, London, 1989) p. 1.
22. S. WEINER and P. A. PRICE, *Calcif. Tiss. Int.* **39** (1986) 365.

Received 3 August

and accepted 14 September 1993